Ergonomics

ISSN: 0014-0139 (Print) 1366-5847 (Online) Journal homepage: https://www.tandfonline.com/loi/terg20

A three-dimensional anthropometric solid model of the hand based on landmark measurements

Matthew S. Rogers , Alan B. Barr , Boontariga Kasemsontitum & David M. Rempel

To cite this article: Matthew S. Rogers , Alan B. Barr , Boontariga Kasemsontitum & David M. Rempel (2008) A three-dimensional anthropometric solid model of the hand based on landmark measurements, Ergonomics, 51:4, 511-526, DOI: 10.1080/00140130701710994

To link to this article: https://doi.org/10.1080/00140130701710994

Published online: 25 Jun 2008.

Ergonomics
Vol. 51, No. 4, April 2008, 511–526

Taylor & Francis
Taylor & Francis Group

A three-dimensional anthropometric solid model of the hand based on landmark measurements

Matthew S. Rogers, Alan B. Barr, Boontariga Kasemsontitum and David M. Rempel*

Ergonomics Program, Department of Bioengineering, University of California, Berkeley, CA, USA

Hand anthropometry data are largely based on measurements of the hand in an outstretched hand posture and are, therefore, difficult to apply to tool gripping hand postures. The purpose of this project was to develop a representative, scalable hand model to be used with 3-D software drawing packages to aid in the ergonomic design of hand tools. Landmarks (66) on the palmar surface of the right hand of 100 subjects were digitised in four functional hand postures and, from these, 3-D surface models of a mean, 25th and 75th% hand were developed. The root mean square differences in hand length between the hand model and the digitised data for the 25th, 50th and 75th percentile hand were 11.4, 3.2 and 8.9 mm, respectively. The corresponding values for hand breadth were 2.0, 0.4 and 1.4 mm. There was good agreement between distances on the digitised hand and the hand model. The application of this research includes improved ergonomic hand tool design through the use of hand anthropometry reference values developed from the general population using grasping hand postures.

Keywords: grasp; computer-aided design; hand, surface; hand tool design

1. Introduction

Ergonomic hand tool design involves optimising the handle to effectively carry out the intended function of the tool with the least load to muscles, tendons, skin and joints. One aspect of this process is to optimise hand–tool contact points in order to maximise grip strength, minimise contact stress with special interest to sensitive areas of the palm and wrist, and provide appropriate tactile feedback. The grip strength is determined by the biomechanical advantage created by finger joint angles as well as the physiological advantage associated with the differences in muscle length (Buchholz and Armstrong 1992). The hand posture and the related grip strength are influenced by the shape of the handle and the hand size. Unfortunately, there are no databases for the tool designer to turn to with the hand in functional hand postures.

The US Army developed large databases of hand anthropometry with the hand in a 'flat' or outstretched posture (Greiner 1992). Data from 'flat' hand databases cannot be easily adapted to tool-holding postures (Armstrong 1982). To develop a functional hand model, Buchholz and Armstrong (1991) used calliper measurements to create ellipsoidal representations of the surface of finger segments then estimated locations of

*Corresponding author. Email: david.rempel@ucsf.edu

ISSN 0014-0139 print/ISSN 1366-5847 online

DOI: 10.1080/00140130701710994
http://www.informaworld.com

finger joint centres using data from radiographs of cadaver hands (Buchholz *et al.* 1992). They integrated this into a 3-D model of the hand designed to interact with tool handles and objects (Buchholz and Armstrong 1992). Two limitations of the model were the lack of a representation of a palmar surface that can interact with a tool and the use of ellipsoids to represent the finger segments. Ellipsoids were used to decrease computer processing time. Other models have been developed to model the four fingers during a power grip (Sancho-Bru *et al.* 2003) or to predict finger positions during a power grasp based on the object shape (Zhang 2005) but these models do not also consider the shape of the palm or thumb during the grasp.

The purpose of this study was to develop a static 3-D model of the palmar surface of the human hand in functional hand postures by digitising the surfaces of hands from 100 people. The database is used to calculate distances between palmar landmarks for different hand postures and determine the variability in distances between hand postures and between hand sizes. The database is also used to develop 3-D models of the human hand, in several hand sizes and postures, which can interact with 3-D models of hand tools using engineering graphing software.

2. Methods

3-D points on the palmar surface of the right hand of subjects were digitised with the hand in four hand postures. Marks were placed on the palmar surface of each subject's hand based on anatomical landmarks. The hand was supported in four hand postures and the marks were digitised and callipers were used to measure linear dimensions. The digitised data and published data were used to create 3-D models of the hand. Dimensions from the 3-D models were compared to the calliper measured dimensions.

2.1. Participants

A total of 107 subjects with no major injury or trauma to their right hand participated in this study. Recruitment was done via flyers distributed in the community and subjects were recruited to represent the gender, age and racial distribution of the San Francisco Bay Area. The study was approved by the Committee on Human Research of the University of California at San Francisco.

2.2. Hand postures

Four hand postures were selected to bracket a range of functional postures for tool design (Figure 1). The postures were selected as extreme possible postures for hand tool use. In the future, these postures will be used, after estimating finger joint centres of rotation, to build hand postures that lie between these extremes. Posture D was added near the end of the study, therefore the sample size is smaller.

Posture A: fingers in relaxed extension and abduction (holding a large ball) ($n = 100$).

Posture B: fingers in relaxed extension in adduction (holding a mouse) ($n = 100$).

Posture C: chuck pinch posture with 2.2 cm ring between tips of digits 1, 2 and 3 ($n = 100$).

Posture D: hand in a power grip posture, similar to holding a tube of approximately 4 cm diameter ($n = 20$).

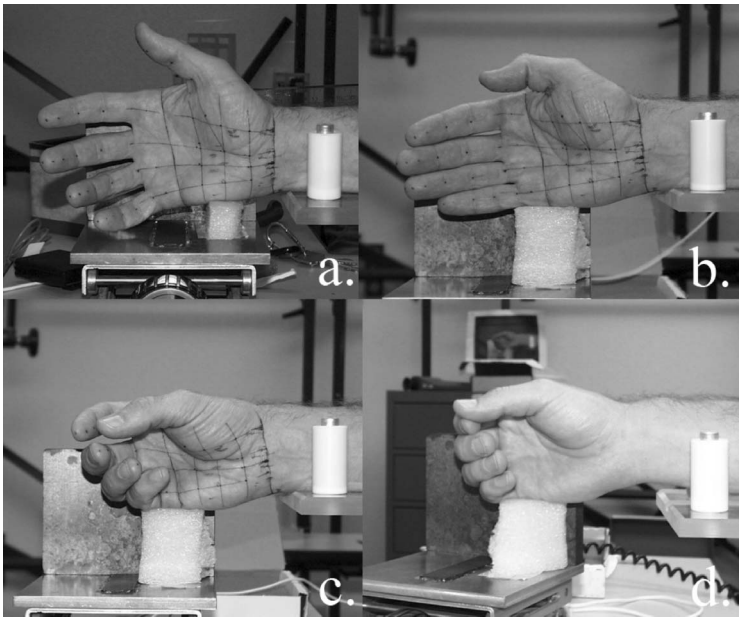

Figure 1. Representative hand postures for point digitisation. (a) Position A: hand-open fingers abducted; (b) position B: hand-open fingers adducted; (c) position C: chuck pinch; (d) position D: power grip.

2.3. Palmar surface landmark digitising

Surface marker points on the hand were selected to represent locations likely for hand–tool contact. The marker locations were also selected with consideration given to ability to calculate joint angles, proper skin lofting and the ability to interpolate to create a complete hand. Locations of higher skin stiffness and lower tissue deformability were selected over locations of lower skin stiffness and higher tissue deformability, e.g. at the joint vs. between joints, to more accurately represent the location of the hand–tool contact position after deformation. The marker scheme is given in Figure 2 (six points on the back or side of the hand are not shown).

A motion analysis system was used to digitise the marks on the hand with a digitising probe. Two camera banks, each with three cameras (Optotrack; Northern Digital Inc., Ontario, Canada) were mounted to a wall between 120 and 180 cm from the hand. The manufacturer stated error is ± 0.1 mm (SD). The measured accuracy and repeatability of the system were ± 0.015 mm and ± 0.009 mm, respectively.

Once the surface points were marked, the subject oriented his or her hand to that in a photograph, with the guidance of the technician. The hand and arm supports were adjusted to support the hand posture and maintain a functional neutral wrist posture (e.g. 15° extension and 0° ulnar/radial deviation). Each surface point was digitised with the sensor probe. The hand posture was then changed to the next posture and the points were again digitised. Digitisation involved applying a very light touch of the probe tip to the hand and therefore almost no tissue deformation.

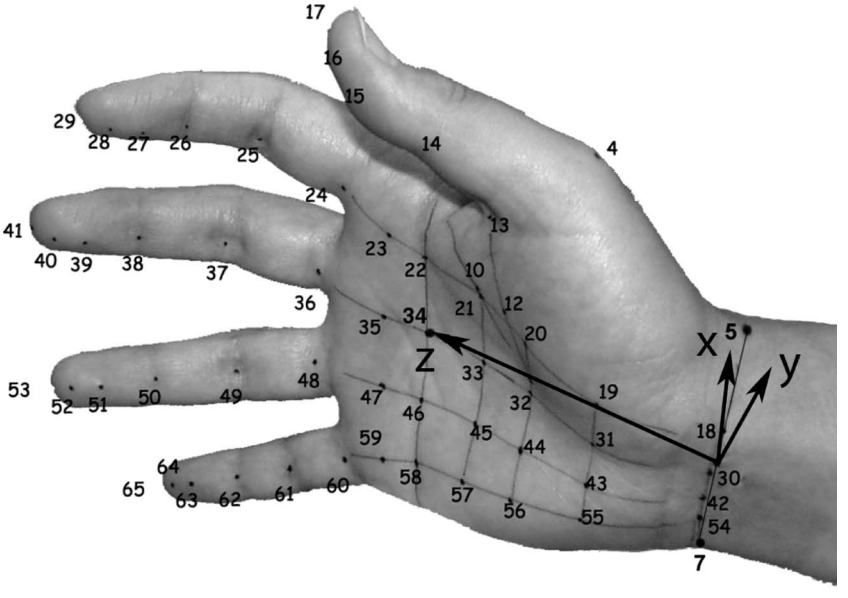

Figure 2. The axis orientation scheme used for the transformation from the room coordinate system to a local coordinate system centred in the wrist. The origin is defined to be near the centre of the wrist, halfway between points 5 and 7. Points 5, 7 and 34 define the x-z plane; the z-axis is defined by the origin and point 34. The x-axis points toward the radial side of the hand and the y-axis is then defined by the right hand rule (it points toward the dorsum of the wrist). A number of points on the back of the hand are not shown: point 1 is at the wrist crease along a projection of the index finger; points 2 and 3 are over the metacarpalphalangeal joints of the index and middle fingers, respectively; point 6 is located on the radial side of digit 2 at the distal palmar crease; point 9 is along the ulnar side of digit 5 at the distal palmar crease (the palmar line between these points falls on points 22, 34, 46, and 58) (the distance between points 6 and 9 is the hand breadth).

2.4. Hand calliper measurements

Subjects completed a demographic questionnaire and the following hand dimensions were measured using a calliper following the directions used for measuring hand anthropometry by the US Army (Greiner 1992).

Arm length: Distance between the back of the tip of the elbow to the tip of the middle finger.

Hand length: Perpendicular distance from the tip of the middle finger to the wrist crease base line.

Hand breadth: Distance between the radial side of metacarpal D2 (index finger) and ulnar side of metacarpal D5 (small finger).

Wrist breadth: Distance between the ulnar side and the radial side of the wrist at the distal wrist crease.

D2, PIP breadth: Distance between the ulnar side and the radial side of the proximal interphalangeal joint crease of the index finger.

D2, PIP depth: Distance between the palmar side and the dorsal side of the proximal interphalangeal joint.

D2, DIP breadth: Distances between the ulnar side and the radial side of the distal interphalangeal joint crease of the index finger.

D2, DIP depth: Distance between the palmar side and the dorsal side of the distal interphalangeal joint.

2.5. Analysis

2.5.1. Data transformation

The palmar surface digitised data were saved in a coordinate system, which was fixed relative to the room. These 'raw' data points were used to calculate distances between landmarks. For the development of a 3-D model of the hand for use in SolidWorks or other computer-aided design (CAD) software, the data points were transformed into a local coordinate system centred at the wrist, summary measures were made across all hands, and surfaces were designed to fit the data.

The origin of the local coordinate system was in the centre of the wrist, midway between points 5 and 7, in a location similar to the wrist centre of rotation (Ryu *et al.* 1991). Point 5 was located at the radial side of the distal wrist crease approximately half way through the thickness of the wrist in a lateral (radial) view. Point 7 was opposite, lying midway along the ulnar side of the wrist, also in line with the distal wrist crease. Points 5, 7 and 34 defined the x-z plane. The positive z-axis projected through point 34, which was located at the intersection of two construction lines (Figure 2). One construction line connected the ulnar and radial side of the transverse palmar crease. The other ran from the midpoint of the wrist crease to the midpoint of the middle finger proximal flexion crease. The positive x-axis was perpendicular to the z-axis and pointed toward the thumb (radial) side of the wrist. The right hand rule defined the y-axis, with the positive y-axis pointed toward the back of the wrist (Figure 2).

A coordinate transformation was performed using the Rigmaker application of Optotrack to transform the 3-D data from the room coordinate system to a local hand coordinate system with the origin at the centre of the wrist. The Rigmaker program uses matrix transformation and three alignment parameters (the origin marker, the axis markers and the cardinal plane markers) to create the local coordinate system. Points 5 and 7 were entered into the original marker field to define the origin. Point 34 was entered into the axis marker field as a marker on the z-axis and points 5 and 7 were entered into the cardinal plane markers as markers on the XZ plane.

2.5.2. Hand model design

The development of hand models involved calculating a mean value for all hand surface points, then using mean calliper measured finger joint dimensions for digit 2 and existing databases to calculate the dimensions of the other fingers and finally fitting surfaces. The first step involved creating the palmar surface of a mean hand for each of the four hand postures using the 66 points (x, y, z) from 100 subjects in their local coordinate system. A mean hand was chosen over a median hand because selecting a median hand based on some dimension, such as hand length, would have meant picking one person's hand to represent all of the dimensions of the hand. Then all other dimensions, for example, the hand breadth, would also be represented by that person's hand even if that dimension was not actually the median of the population. Furthermore, the x, y and z values for all points were relatively normally distributed. The mean and standard deviation for the x, y and z location of each of the 66 points were calculated across all subjects for each hand posture. The 25th and 75th percentile for each of the 66 points was calculated using the following equation:

$$\text{Desired percentile} = \text{mean} \pm \sqrt{2} erf^{-1}(CI) * \sigma$$

where erf is the error function and σ the standard deviation.

For the 75th percentile, 75% of all subjects would have values that are less than this calculated location. This method can be used to create any desired hand percentile, but it should be noted that as the percentile reaches the extremes, for example, the 99th percentile, small errors in the standard deviation calculations create large changes in measurements. Therefore, the model was built in the 25th to 75th percentile range. Note that this is not a 25th to 75th percentile range built upon a single person's hand measurement, but truly a 50% CI symmetric and centred about the mean hand.

The design of the finger and palm surfaces used data from the surface markers, manual hand measurements of subjects and data from existing databases (Greiner 1992). The data were not separated by gender, but instead grouped, because the current hand tool design process is usually done to identify a single design that will accommodate both genders. As noted above, DIP and PIP breadth and depth were measured with callipers on only digit 2 of all subjects. DIP and PIP breadth and depth for digits 3 to 5 were calculated as ratios of digit 2 (Table 1), which were calculated from the Greiner database (Greiner 1992). The same method was used for the interphalangeal joint. The metacarpophalangeal (MCP) joint depth was extended from a linear equation connecting the DIP depth and the PIP depth with regard to their relative distances from the MCP joint. The MCP breadth was the same as the PIP breadth. Since the palmar surface of the MCP joint is defined by the digitised data points and splines, the purpose of calculating a MCP depth was to generate the locations of the dorsal surface of the MCP joints (knuckles). Fingertips were approximated as an ellipse, centred on the digitised fingertip, with a depth of 2.5 mm and an eccentricity equal to that of the DIP. The fingertip creation required a finite circumference for the tip to allow a rounded connection with the DIP; otherwise, the tip would have been modelled as a cone.

The fingers were designed as three tapering cylinders of elliptical cross-section dependent on the joint conditions. For example, segment 2 (between the DIP and the PIP joint) of the finger is built as a cylinder with one elliptical end cap determined by the PIP and the other by the DIP. 3-D models have been constructed using a method of overlapping ellipsoids (Buchholtz and Armstrong 1991). The cylinder method was chosen instead of the overlapping ellipsoids for three reasons. First, the ellipsoid method does not accurately represent the breadth of the phalange segment. Second, no information is available to suggest a suitable eccentricity for the ellipse or the variance between hand sizes or digits. Third, the ellipsoid method does not take into account the change of eccentricity as the joint angle increases. The palmar surface of a segment of an extended finger has very little proximal to distal curvature; but has increasing curvature as the finger is flexed. The method developed with the cylinder model allows for future modifications incorporating a change in finger eccentricity as the joint angles change using a series of guide curves and lofts.

Table 1. The ratio of joint depth and breadth of the Nth digit in relation to that of the second digit from the US Army database (Greiner 1992).

	Digit 3/Digit 2	Digit 4/Digit 2	Digit 5/Digit 2
DIP breadth	1.00	0.93	0.85
DIP depth	1.03	0.97	0.88
PIP breadth	1.01	0.94	0.82
PIP depth	1.03	0.97	0.86

Note: These factors were used to calculate joint dimensions for digits 3, 4 and 5 from the dimensions measured from digit 2 for each subject.
DIP = distal interphalangeal; PIP = proximal interphalangeal.

2.5.3. Creation of the hand models

SolidWorks Office (SolidWorks, Concord, MA, USA), a 3-D CAD program was used to build the solid models of the hand. Parametrically fitted splines were used to interpolate between relevant points. Relevant points are those points that move together when a finger joint is flexed or extended. For example, the points at the end of the finger, distal to the DIP joint are connected using splines, but the points on either side of the DIP or PIP joint are not. This allows the creation of creases and links digit segments that have similar shapes between hand postures. The DIP joint can flex with little or no change in the tip pad. The fitted splines or guide curves are listed in Table 2. The palmar surface is created by fitting lofts between these guide curves. A loft is the curved surface fit to a set of points in three dimensions. For example, lofting a surface between the closed curves built by 5, 18, 30, 42, 54, 7, 1 and 9, 58, 46, 34, 22, 6, 2, 3 creates a coarse palm. Then the specific contours and shape of the palm are created by adding the rest of the palmar splines listed in Table 2. The fingers are built using the data derived for the PIP, DIP and fingertip dimensions. A spline running along the points on the palmar surface of each digit is created and used to define a plane normal to the spline at each joint location, specifically points 24–29 for digit 2, 36–41 for digit 3, 48–53 for digit 4 and 60–65 for digit 5. The point located on the dorsal side of the hand at the MCP joint of digit 2 (point 2) and the point on the palmar side of the hand where digit 2 intersects the palmar crease, point 22, define a line perpendicular to the axis about which flexion and extension take place. This line and the plane perpendicular to the spline running through the points on the palmar side of the phalange fully define the ellipse, which is used to create the PIP, DIP and fingertip. Guide curves, which connect the minor-minor and major-major axis of each ellipse, allow the creation of cylinder-based phalanges. The region connecting the phalanges to the palm is simulated by extending a loft from the base of the phalange to the adjacent digit at the palmar crease. For example, the elliptical base of digit 2 located at point 24 is guided by a curve from the outside of the ellipse to point 35. This serves to create a web surface at the base of the fingers whose width is dependent on the relative abduction, adduction, flexion and extension between adjacent digits. Non-adjacent digits are unaffected by displacement.

Table 2. A list of points used to make the 21 splines that create the guide curves that serve as a wire frame for creating surfaces of the hand.

Palmar splines	Phalange splines
5, 18, 30, 42, 54, 7, 1, 5	24, 25, 26, 27, 28, 29
9, 58, 46, 34, 22, 6, 2, 3, 9	36, 37, 38, 39, 40, 41
54, 55, 56, 57, 58	48, 49, 50, 51, 52, 53
42, 43, 44, 45, 46	60, 61, 62, 63, 64, 65
20, 21, 22, 23, 24	6, 22, 33, 31, 18, 5, 1, 6
58, 59, 60	13, 21, 33
46, 47, 48	top of MCP circle, 20, 32
24, 25, 26	top of MCP circle, 19, 31
7, 8, 9	4, 5
5, 6	14, 15, 16, 17
1, 2	

Note: The parametric splines are of the same order as the number of points used to define the spline.
MCP = metacarpophalangeal.

2.5.4. Validation

A comparison of root mean square (RMS) distance between important landmarks digitised to calliper measurements on a per subject and percentile basis was used to validate the digitisation process. The median landmark distances are compared to the mean because the model is built from a mean hand. The model was compared to both the digitised and calliper measurements.

3. Results

3.1. Participants

Data points were collected from 107 subjects, of which 89 produced unflawed position measurements for all hand postures after digitisation. Of the remaining subjects, 11 had datasets with one or two missing points (of 264 points for each person); these missing points were replaced by an average from the 89 good datasets scaled to the length of that subject's hand. This resulted in a full dataset for 100 subjects (50 male and 50 female) aged 19–64 years (35.6 $\pm$ 14.6; mean $\pm$ SD) for hand postures A, B and C and 20 subjects for hand posture D. The participants' mean height was 168.9 $\pm$ 8.9 cm and mean weight was 73.5 $\pm$ 28.4 kg. The ethnicity distribution of the participants in comparison to the San Francisco Bay area ethnicity is 30%:19%, 10%:8%, 8%:19%, 0%:0.6%, 49%:58%, 3%:9.2% Asian, Black, Latino, Native American, White and other, respectively. The distribution of study participant ages to San Francisco Bay Area ages is 26%:12%, 23%:17%, 25%:17%, 13%:14%, 13%:8% for ages 18–24, 25–34, 35–44, 45–54 and 55–64 years, respectively (Census 2000).

3.2. Hand calliper measurements

The distances between hand landmarks, based on manual measurements made using the callipers prior to digitisation, and following the definitions used for the US Army database (Greiner 1992), are presented in Table 3.

3.3. Hand models

Representative 3-D hand models were built for a 25th, mean and 75th percentile hand in all four functional hand postures (Figures 3, 4 and 5). The figures for posture D are based on data from 20 subjects. The four hand postures can be characterised by the angles of the

Table 3. Summary measures of distances (mm) on the flat hand measured using callipers following the methods of Greiner (1992) (n = 100).

Landmarks	Mean (SD)	10%	25%	50%	75%	90%
Hand length	178.1 (13.5)	160.0	168.0	177.0	186.0	195.0
Hand breadth	84.5 (7.5)	74.0	78.0	85.0	90.0	94.0
Wrist breadth	59.1 (5.5)	53.0	54.5	58.0	64.0	66.5
Proximal interphalangeal width	19.4 (2.0)	17.0	18.4	19.0	21.0	22.0
Proximal interphalangeal depth	17.8 (2.0)	15.5	17.0	17.5	19.0	20.0
Distal interphalangeal width	17.0 (1.9)	15.0	16.0	17.0	18.0	19.0
Distal interphalangeal depth	14.0 (1.6)	12.0	13.0	14.0	15.0	16.0
Arm length	456.1 (32.6)	416.0	434.0	453.0	476.0	495.0

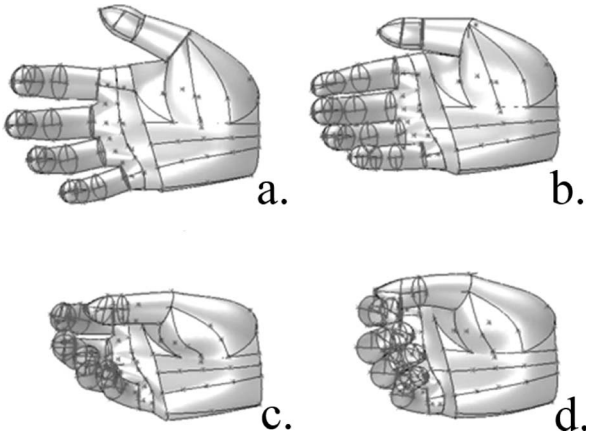

Figure 3. The mean hand model in postures A, B, C and D.

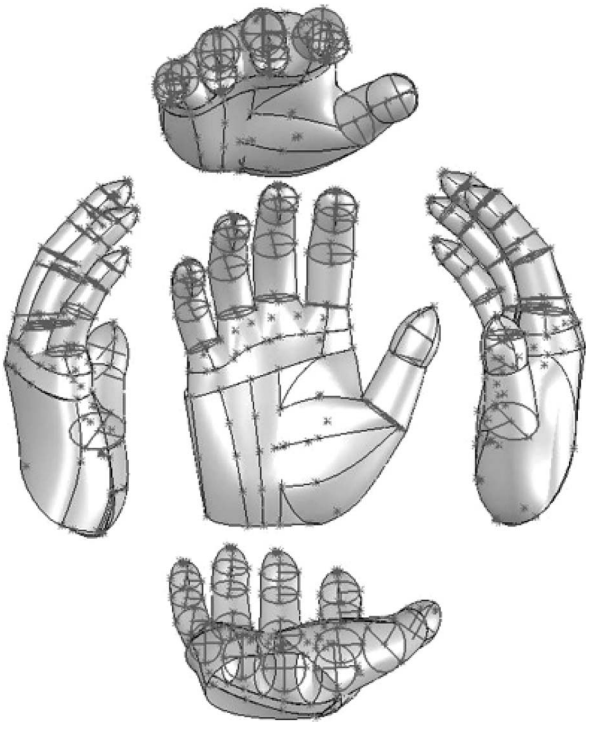

Figure 4. Hand model in posture B rotated to allow multiple views.

finger joints. The mean angles of the DIP joints, PIP joints and MCP joints for each hand posture are presented in Table 4.

3.4. Validation

Calculated distances between some hand landmarks from the raw digitised data by population percentile are presented in Table 5. The raw digitised data points were also

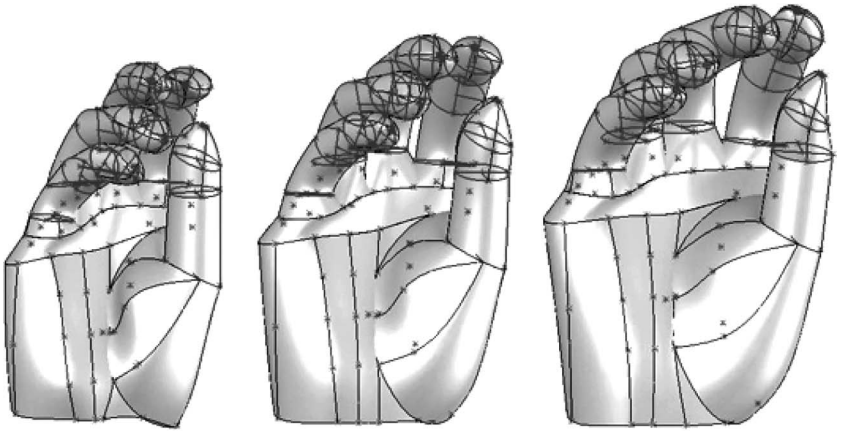

Figure 5. The hand model built as a 25th, mean and 75th percentile representation for posture C.

Table 4. The mean (SD) of the angles of the interphalangeal (IP) joint, metacarpophalangeal (MCP) joints, proximal interphalangeal (PIP) joints and distal interphalangeal (DIP) joints.

	Mean joint angles in degrees (SD)			
	Posture A	Posture B	Posture C	Posture D
Digit 1: IP				
IP	174.0 (14.8)	162.9 (16.2)	172.3 (17.1)	168.4 (8.8)
Digit 2:				
MCP	162.6 (7.9)	155.6 (6.2)	142.5 (14.2)	145.5 (7.9)
PIP	161.3 (8.6)	171.4 (6.4)	157.8 (12.9)	123.6 (12.6)
DIP	171.7 (5.8)	175.6 (4.8)	170.4 (12.0)	150.0 (7.8)
Digit 3:				
MCP	156.0 (7.1)	152.7 (6.2)	138.5 (15.3)	130.7 (7.4)
PIP	161.6 (9.4)	167.1 (9.6)	151.8 (11.2)	127.8 (10.8)
DIP	171.7 (6.8)	175.2 (4.9)	163.1 (11.7)	145.2 (10.9)
Digit 4:				
MCP	154.9 (7.5)	158.0 (7.0)	136.8 (15.5)	133.3 (7.7)
PIP	160.0 (10.3)	167.1 (10.5)	146.7 (12.9)	124.1 (10.7)
DIP	171.8 (9.4)	174.4 (6.2)	161.5 (18.7)	148.0 (10.6)
Digit 5:				
MCP	159.3 (8.5)	159.5 (7.5)	140.6 (17.9)	144.9 (9.7)
PIP	166.8 (12.7)	175.9 (7.4)	161.6 (17.1)	131.7 (11.4)
DIP	168.3 (10.2)	173.2 (6.3)	158.7 (15.6)	137.6 (13.3)

Note: The angles were determined first for each subject from their digitised data then averaged across subjects.

used to calculate distances between the centre of the index fingertip pad (point 27) and the centre of the other digit pads (points: thumb 15; middle 39; ring 51; small 63) (Table 5a,b) and between a point on the thenar wad (point 21) and the index finger pad (point 27) and thumb finger pad (point 15) (Table 5b).

Some of the same distances between landmarks in Table 5 (raw digitised data) were also calculated from the hand models (Table 6). These distances are compared to the calliper measured and raw digitised data in Figure 6. The differences between the calliper measured data vs. the data from the digitised hand (posture A) for hand length are 6.6 mm

Table 5a. Distances (mm) between raw digitised landmarks on the fingertips: thumb pad (point 15), index finger pad (27), middle finger pad (39), ring finger pad (51) and small finger pad (63) plus hand length, breadth and wrist breadth.

Posture	Landmarks	Mean (SD)	10%	25%	50%	75%	90%
	Hand length	175.1(12.7)	158.1	164.5	175.0	183.6	189.7
	Hand breadth	82.8 (7.2)	72.2	77.3	82.8	88.5	92.6
	Wrist breadth	61.1 (5.4)	54.4	56.5	60.5	65.4	68.1
A	15–27	67.5 (14.7)	48.1	57.4	66.3	75.4	88.3
	27–39	31.0 (7.8)	21.4	25.3	30.3	34.4	40.5
	39–51	27.2 (7.1)	19.9	21.2	26.4	31.5	36.6
	51–63	31.4 (7.2)	22.4	26.3	30.7	35.1	41.2
B	15–27	60.1 (10.6)	47.7	54.6	59.8	66.1	71.0
	27–39	20.7 (3.4)	17.0	18.0	20.4	22.5	25.0
	39–51	18.0 (3.0)	14.4	15.9	17.7	19.3	21.0
	51–63	22.8 (4.6)	17.3	19.4	22.7	25.4	28.3
C	15–27	22.3 (4.8)	16.1	19.0	22.3	25.3	29.4
	27–39	18.7 (4.1)	13.9	16.5	18.0	21.1	23.5
	39–51	20.0 (6.3)	11.8	15.7	18.9	23.3	28.5
	51–63	17.2 (4.7)	12.0	13.7	16.3	19.4	23.3
D	15–27	9.1 (4.8)	4.6	6.0	7.2	11.2	14.8
	27–39	17.4 (2.5)	14.3	15.5	17.1	18.8	21.1
	39–51	17.0 (2.8)	13.1	14.9	15.9	19.4	21.0
	51–63	15.9 (4.3)	11.8	13.8	14.9	17.1	19.3

Table 5b. Distances (mm) between raw digitised index finger pad (point 27) and the ring finger pad (51) and small finger pad (63). Distances between a point on the thenar wad (point 21) and the index finger pad (27) and the thumb finger pad (point 15).

Posture	Landmarks	Mean (SD)	10%	25%	50%	75%	90%
A	27–51	52.6 (10.7)	39.3	44.8	51.8	58.5	65.9
	27–63	76.6 (14.4)	58.9	65.8	75.1	86.2	94.9
	21–27	88.9 (9.8)	74.8	83.0	89.1	95.2	101.0
	21–15	56.9 (7.9)	46.7	50.6	57.8	61.5	67.1
B	27–51	35.5 (4.9)	42.5	38.1	35.1	32.3	30.1
	27–63	51.8 (6.9)	44.6	47.3	51.1	55.3	59.4
	21–27	86.2 (8.5)	74.5	81.5	86.2	91.8	96.6
	21–15	46.2 (8.6)	35.0	40.4	45.8	51.7	56.5
C	27–51	35.1 (7.4)	27.3	30.2	33.3	38.3	44.4
	27–63	48.1 (10.0)	35.2	41.1	47.2	53.6	61.6
	21–27	65.2 (5.9)	57.0	61.5	65.6	68.7	72.0
	21–15	49.3 (6.6)	40.0	45.0	49.4	54.8	57.2
D	27–51	33.3 (4.6)	28.0	30.0	33.4	35.3	41.0
	27–63	47.6 (6.1)	39.6	43.2	46.0	51.5	55.7
	21–27	45.0 (6.7)	37.8	39.1	43.8	51.2	55.4
	21–15	45.5 (4.8)	39.2	42.7	45.5	47.3	52.4

RMS, 5.6 mm SD, 26.3 mm maximum difference and 0.04 mm minimum difference. The corresponding values for hand breadth are 3.3, 3.4, 25.4 and 0.2 mm and for wrist breadth are 6.7, 4.8, 19.4 and 0.001 mm. A comparison of the hand model length to the digitised data hand length gives a difference of 11.4 mm for the 25th percentile hand, 3.2 mm for

Table 6. Distances (mm) between landmarks on the hand models. These can be compared to raw digitised distances (Table 5): thumb pad (point 15), digit 2 pad (27), a point on the thenar wad (21), the centre of the wrist (30) and middle finger pad (39).

Posture	Landmarks	25%	50%	75%
	Hand length	153.1	171.7	192.6
	Hand breadth	75.3	82.4	89.9
	Wrist breadth	57.2	61.0	64.8
A	15–27	58.8	63.2	67.6
	15–21	46.9	53.7	61.7
	30–15	101.2	110.9	121.6
	30–27	138.3	148.6	159.2
	30–39	139.7	151.5	163.9
B	15–27	53.2	57.6	62.0
	15–21	42.6	45.1	48.5
	30–15	99.7	107.0	114.7
	30–27	137.0	146.7	156.6
	30–39	137.3	148.9	160.9
C	15–21	43.8	47.9	52.2
	30–15	93.2	103.2	113.1
	30–27	112.2	122.3	132.4
	30–39	108.6	118.3	128.0
D	15–21	41.6	44.7	47.9
	30–15	96.5	104.9	113.3
	30–27	94.3	104.3	114.3
	30–39	88.1	97.9	107.8

the 50th percentile hand and 8.9 mm for the 75th percentile hand. The corresponding differences for hand breadth are 2.0, 0.4 and 1.4 mm and for wrist breadth 0.6, 0.3 and 0.5 mm.

4. Discussion

3-D models of the palmar surface of the human hand in four functional hand postures were developed from data digitised from the hands of 100 people. The recruited subjects were similar to the regional population in stature, gender, ethnicity and age; therefore, the data should be generalisable to the larger population. When compared to the hand dimensions from the US Army data on men, this study has smaller hand dimensions on average due to the fact that data from both genders are combined in one dataset. This study has an average hand length of 178.7 mm, while the US Army male population has a mean hand length of 197.2 mm. Mean study hand breadth to mean army hand breadth is 84.8 to 89.6 mm, and study to army wrist breadth is 59.0 to 67.8 mm.

On average, the distances measured using callipers are 6.7 to 3.3 mm greater for hand length and hand breadth (Figure 6) than measurements from the digitised raw data. For wrist breadth, the distances are 6.7 mm less. The differences in hand breadth between the calliper measurements and the digitised values can be attributed to breadth measurement at the MCP joint (calliper) vs. measurement at the distal palmar crease (digitised). The other systematic differences can be attributed to differences in the hand postures during calliper measurement, the flat hand following methods of the US Army, and the digitised measurements, posture A in which the hand is relaxed and the fingers are slightly curved.

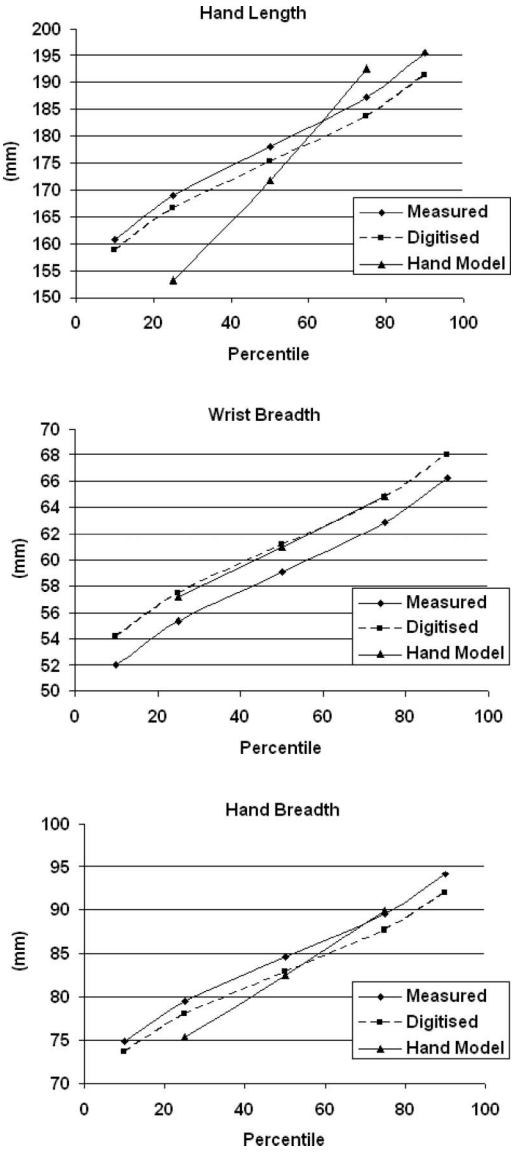

Figure 6. A comparison of calliper measured, raw digitised, and hand model measurements for hand length, wrist breadth and hand breadth. Note that calliper measured data were taken on a flat hand posture while the digitised and model data were taken on hand posture A.

Posture A has shorter distances for hand length compared to an outstretched hand. There is little difference in wrist breadth between calliper measured and raw digitised data. The variability in measurements demonstrates the importance of accounting for hand posture when using data and highlights the need for a database with the hand in functional postures.

Another source of variability was the between-subject reliability in positioning the hand for each of the hand postures. Since the palmar surface data between subjects were transformed to an axis based on wrist and palm markers, the primary variability will be in

the fingers due to differences in finger positioning between subjects. The magnitude of this variability is indicated by the standard deviation of finger flexion angles between subjects within a hand posture (columns in Table 4). Across all fingers and joints, the mean coefficients of variability (SD/mean) for postures A, B, C and D were 0.06, 0.05, 0.10 and 0.07, respectively. These indicate good reproducibility of postures, although posture C had greater between-subject variability than the other postures.

Verification of the hand model was done by comparing measurements from the 3-D hand models to digitised raw data. Each hand model is built from 66 points averaged across 100 subjects (postures A, B, C) following a series of rules. The models, therefore, are representative of data from the subjects but not a perfect match. The accuracy of the models is best for distance measurements that are close to the origin. Distances near the origin are preserved, while distances far from the origin are not. For example, agreement on wrist breadth is excellent (Figure 6b) because this measurement lies along the x-axis through the origin. Figure 6a demonstrates the error introduced by measurements far from the origin. This error is introduced because the models were generated from mean subject data that were aligned at the origin, the centre of the wrist. Therefore, measurements made far from the origin will be influenced more by differences between subjects in finger postures and hand shapes. Other hand models could be created from the raw data with the origin in a different location, for example, in the centre of the palm at point 34. This would preserve distance measurements near that point. Using the raw database of digitised data provides the most accurate estimates of distances between points, since distances of interest can be measured on every subject and analysed separately.

Designers of hand tools may be interested in a variety of tool–hand interactions. For example, locating a trigger or switch that is activated by the index finger may require consideration of how the tool fits into the palm. Some of the distances that may influence optimal switch location are index finger pad to the palmar crease, thumb pad to the palmar crease and thumb pad to the index finger pad. For example, if the handle shape fits hand posture D, then the width of the handle, that is, the distance from where the handle contacted the thenar muscle wad between the thumb and the index finger (point 21) and the front edge of trigger, where it was pressed by the index finger (point 27), would be 43.8 mm to accommodate the 50th% (Figure 5b). More importantly, it can be seen that to accommodate the 25th to 75th% of the population this dimension would be between 39.1 mm and 51.2 mm. Another example of the use of these tables is in the design of a keyboard that has a dome shape support surface for the palm and a single button under each finger with a hand shape similar to posture A. The distances between the fingertips, for this posture, for the 25th% and 75th% of the population, could be obtained from Table 5a,b.

Besides using this tabular approach, which summarises important distances in a table, a 3-D engineering program (e.g. SolidWorks) could be used to identify interference points between a tool/object and the hand. For example, a virtual tool could be moved into the palm of the hand model until the tool model contacts the palmar surface of the hand. The contact points on the palm could also be interpreted relative to the regions that are known to be sensitive to contact pressure (Fransson-Hall and Kilbom 1993). After positioning the tool in the palm, the finger contact points on the tool could be identified. This exercise could be repeated for a variety of hand sizes in order to accommodate as many users as possible. Currently, this process is restricted to just the four hand postures digitised. Ultimately, the model will be modified to allow finger flexion about joint centres of rotation.

Distances between key landmarks on the hand in functional hand postures are useful for hand tool design and are unavailable from other data sources. Known as case selection (Human Factors and Ergonomics Society 300 Committee 2004), guidelines have been established for choosing realistic combinations of lengths between landmarks of interest for design purposes. However, without a large database for the hand, in functional postures, this method cannot be used for complicated hand–tool interactions. Therefore, the design of a tool incorporating multiple features calls for a scalable hand built in a functional posture from which multiple measurements can be made. To improve the accuracy of the hand model presented in this paper, multiple hand models could be built, each with an origin corresponding to a different point of interest on the hand. Distances could then be calculated from these origins to other points of interest.

Several limitations of the hand model should be noted. While accurately representing the mean hand, the model may encounter problems in extreme dimensions, especially for hand posture D, which was developed from just 20 subjects. Hand posture D has an overlap of digit 1 and digit 2 of up to 4.8 mm. This occurs because the model does not incorporate the deformation of the fingertip pulp due to a load. For simplicity, the general spline and curve fit was used to create each digit, disregarding the non-linear response of the fingertip deformation to load (Serina *et al*. 1998). Likewise, the decreasing eccentricity of finger segments 2 and 3 with flexion has also been neglected. In addition, confidence in the model decreases at extremes of hand percentiles. Future work on the model could involve adding the non-linear skin stiffness and deformation on contact. Skin response to load can be predicted by adding a viscoelastic model with force relaxation (Jindrich *et al*. 2003). Incorporating the skin stiffness into the model would allow for a more accurate determination of hand tool contact areas. Another limitation is that the current model can only be used in the four hand postures that were digitised. Dynamic finger motion may be possible with the addition of joint centres of rotation (Buchholz *et al*. 1992, Zhang *et al*. 2003). This dynamic interaction would allow the wrapping of the fingers around an arbitrary shape after tool palmar contact has been established. The addition of joint centres of rotation would also permit generating a sequence of static hand postures between the postures digitised.

In conclusion, a scalable hand model in four functional postures has been created based on 3-D hand surface data collected from 100 subjects (20 subjects for posture D). A method for model creation, dependent upon palmar surface landmarks of interest, has been developed. One particular hand model has been created and analysed to demonstrate the strengths and weaknesses of this approach. The hand model allows for a better understanding of changes in the hand surface as the hand posture is changed. In addition, with the hand model, multiple representative distances on the hand can be used, without conflict or the complicated use of case selection. With a 3-D modelling program, hand–tool contact points can be identified across a range of hand sizes in the four functional hand postures collected in this study.

References

Armstrong, T.J., 1982. Development of a biomechanical hand model for study of manual activities. *Anthropometry and biomechanics: Theory and application*. New York: Plenum, 183–191.

Buchholz, B. and Armstrong, T.J., 1991. An ellipsoidal representation of human hand anthropometry. *Human factors*, 33, 429–441.

Buchholz, B. and Armstrong, T.J., 1992. A kinematic model of the human hand to evaluate its prehensile capabilities. *Journal of biomechanics*, 25, 149–162.

Buchholz, B., Armstrong, T.J., and Goldstein, S.A., 1992. Anthropometric data for describing the kinematics of the human hand. *Ergonomics*, 35, 261–273.

Fransson-Hall, C. and Kilbom, A., 1993. Sensitivity of the hand to surface pressure. *Applied ergonomics*, 24, 181–189.

Greiner, T.M., 1992. *Hand anthropometry of U.S. army personnel*. NATICK/TR-92/011(technical report). Natick, MA: US Army Natick, Research, Development & Engineering Center.

Human Factors and Ergonomics Society 300 Committee, 2004. *Guidelines for using anthropometric data in product design*. Santa Monica, CA: Human Factors and Ergonomics Society.

Jindrich, D.L., Zhou, Y., Becker, T., and Dennerlein, J.T., 2003. Non-linear viscoelastic models predict fingertip pulp force-displacement characteristics during voluntary tapping. *Journal of biomechanics*, 36, 497–503.

Lee, S.W. and Zhang, X., 2005. Development and evaluation of an optimization-based model for power-grip posture prediction. *Journal of biomechanics*, 38, 1591–1597.

Ryu, J., Palmer, A.K., and Cooney, W.P., 1991. Wrist joint motion. *In*: K.N. An, R.A. Berger, and W.P. Cooney, eds. *Biomechanics of the wrist joint*. New York: Springer Verlag.

Sancho-Bru, J.L., Perez-Gonzalez, A., Vergara, M., and Giurintano, D.J., 2003. A 3D biomechanical model of the hand for power grip. *Journal of biomechanical engineering*, 125, 78–83.

Serina, E.R., Mockensturm, E., Mote, C.D. Jr, and Rempel, D., 1998. A structural model of the forced compression of the fingertip pulp. *Journal of biomechanics*, 31, 639–646.

US Census Bureau, 2000. Census Data, Census 2000. Available from: www.bayareacensus.ca.gov [Accessed 10 October, 2005], Association of Bay Area Governments.

Zhang, X., Lee, S.W., and Braido, P., 2003. Determining finger segment centers of rotation in flexion-extension based on surface marker measurement. *Journal of biomechanics*, 36, 1097–1102.